Table 1. Pumping rates of larvae and adults treated with respiratory chain RNAi.

RNAi treatment	Feeding rate (pumps per minute)*			
	Day 2	Day 3	Day 4	Day 5
Vector	118 ± 15 (0/8)	140 ± 21 (0/8)	145 ± 24 (0/8)	131 ± 49 (1/10)
Complex III (*cyc-1*) larval + adult	97 ± 21 (0/10)	83 ± 12 (0/10)	84 ± 12 (0/10)	75 ± 12 (0/10)
Complex III (*cyc-1*) adult only	79 ± 62 (5/12)	112 ± 80 (3/12)	80 ± 59 (4/12)	69 ± 45 (4/12)
Complex V (*atp-3*) larval and adult	98 ± 15 (0/10)	87 ± 10 (0/10)	80 ± 9 (0/10)	75 ± 8 (0/10)
Complex V (*atp-3*) adult only	88 ± 80 (6/14)	98 ± 64 (5/14)	83 ± 59 (4/14)	89 ± 54 (4/14)

*Mean ± SD. The number of pharyngeal pumps observed in an adult animal in 1 min at 25°C. Number in parentheses is the number of animals that produced fewer than 50 pumps per minute/total number of animals tested.

longer than normal. This lack of life-span extension was particularly unexpected because mitochondrial respiration is widely assumed to influence aging in an ongoing manner during adulthood through the generation of reactive oxygen species (*8*, *20*). Our findings bring this assumption into question.

Caloric restriction during adulthood extends life-span and has been proposed to act by decreasing the rate of respiration (*21*, *22*). However, our finding that life-span extension caused by respiratory-chain RNAi requires inhibition during development suggests that caloric restriction in animals, as in yeast (*23*), extends life-span in another way. The same holds for insulin/IGF-1 signaling, which functions exclusively during adulthood to influence *C. elegans* life-span (*19*).

In conclusion, we propose that *C. elegans* possesses a regulatory system that senses, interprets, and remembers the rate of mitochondrial respiration during development. Under normal conditions, this system establishes normal rates of growth, behavior, and aging. However, if the rate of respiration is low, this system reduces the animal's growth rate and body size, as well as its rates of behavior and aging. It is possible that the rate of respiration during development is sufficient to specify the rate at which the animal lives its entire life; alternatively, the adult animal may make reference to contemporaneous rates of respiration, which, in turn, are influenced by mitochondrial activity during development.

References and Notes

1. A. G. Fraser *et al.*, *Nature* **408**, 325 (2000).
2. A. Dillin, D. Garigan, C. Kenyon, unpublished data.
3. Materials and methods are available as supporting material on *Science* Online.
4. E. C. Slater, *Trends Biochem. Sci.* **8**, 239 (1983).
5. J. E. Sulston, H. R. Horvitz, *Dev. Biol.* **56**, 110 (1977).
6. M. Estevez *et al.*, *Nature* **365**, 644 (1993).
7. H. A. Tissenbaum, L. Guarente, *Nature* **410**, 227 (2001).
8. J. Feng, F. Bussiere, S. Hekimi, *Dev. Cell* **1**, 663 (2001).
9. A. Wong, P. Boutis, S. Hekimi, *Genetics* **139**, 1247 (1995).
10. B. Lakowski, S. Hekimi, *Science* **272**, 1010 (1996).
11. H. Miyadera *et al.*, *J. Biol. Chem.* **276**, 7713 (2001).
12. T. Jonassen, P. L. Larsen, C. F. Clarke, *Proc. Natl. Acad. Sci. U.S.A.* **98**, 421 (2001).
13. B. P. Braeckman, K. Houthoofd, A. De Vreese, J. R. Vanfleteren, *Curr. Biol.* **9**, 493 (1999).
14. L. Guarente, C. Kenyon, *Nature* **408**, 25 (2000).
15. W. A. Van Voorhies, S. Ward, *Proc. Natl. Acad. Sci. U.S.A.* **96**, 11399 (1999).
16. D. Gems *et al.*, *Genetics* **150**, 129 (1998).
17. R. F. Ketting *et al.*, *Genes Dev.* **15**, 2654 (2001).
18. S. W. Knight, B. L. Bass, *Science* **293**, 2269 (2001).
19. A. Dillin, D. K. Crawford, C. Kenyon, *Science* **298**, 830 (2002).
20. D. Harman, *Mutat. Res.* **275**, 257 (1992).
21. M. R. Klass, *Mech. Ageing Dev.* **6**, 413 (1977).
22. L. W. Means, J. L. Higgins, T. J. Fernandez, *Physiol. Behav.* **54**, 503 (1993).
23. S. J. Lin *et al.*, *Nature* **418**, 344 (2002).

24. We thank Kenyon lab members for discussions and comments on the manuscript. A. D. was supported by the Damon Runyon Cancer Research Fund (DRG-1525). A-L.H. was supported by the Canadian Institutes of Health Research. N.A.O. was supported by The Portuguese Foundation for Science and Technology and the Gulbenkian Foundation. This work was supported by a grant from the Ellison Foundation to C.K.

Supporting Online Material
www.sciencemag.org/cgi/content/full/1077780/DC1
Materials and Methods
Figs. S1 and S2
Tables S1 and S2

27 August 2002; accepted 14 November 2002
Published online 5 December 2002;
10.1126/science.1077780
Include this information when citing this paper.

Coordinated Nonvectorial Folding in a Newly Synthesized Multidomain Protein

Annemieke Jansens,* Esther van Duijn, Ineke Braakman†

The low-density lipoprotein receptor (LDL-R) is a typical example of a multidomain protein, for which in vivo folding is assumed to occur vectorially from the amino terminus to the carboxyl terminus. Using a pulse-chase approach in intact cells, we found instead that newly synthesized LDL-R molecules folded by way of "collapsed" intermediates that contained non-native disulfide bonds between distant cysteines. The most amino-terminal domain acquired its native conformation late in folding instead of during synthesis. Thus, productive LDL-R folding in a cell is not vectorial but is mostly posttranslational, and involves transient long-range non-native disulfide bonds that are isomerized into native short-range cysteine pairs.

In eukaryotic cells, multidomain proteins are thought to fold their domains independently and sequentially (*1–3*). Examples of multidomain proteins have been found in the LDL-R family, which consists of a range of receptors that share structural elements (*4, 5*). The LDL-R itself is a surface glycoprotein that mediates cellular uptake of LDL (*6*). It has been proposed that its ectodomain consists of three regions (Fig. 1A): the NH_2-terminally located ligand-binding region (composed of seven complement-like domains, each stabilized by three disulfide bonds and a calcium ion) (*7, 8*), the epidermal growth factor (EGF) precursor-like region (*9, 10*), and the abundantly O-glycosylated region. Structure determinations and in vitro folding studies of LDL-R fragments indicated a linear domain organization (Fig. 1A). This result suggests independent and sequential folding of the ligand-binding domains in the complete LDL-R (*11, 12*).

Protein folding in the endoplasmic reticulum (ER) is tightly linked with disulfide bond formation in the newly synthesized protein (*13, 14*). Whether non-native disulfide bonds are abundant or even essential in a folding pathway is still a matter of debate. Non-native bonds appear frequently in folding assays in vitro (*15–17*), but their occurrence in productive folding pathways in intact cells may be bypassed by the activity of protein

Department of Bio-Organic Chemistry 1, Bijvoet Center for Biomolecular Research, University of Utrecht, Padualaan 8, 3584 CH Utrecht, Netherlands.

*Present address: Biological Sciences, Stanford University, 325 Serra Mall, Stanford, CA 94305, USA.
†To whom correspondence should be addressed. E-mail: i.braakman@chem.uu.nl

disulfide isomerases (*16, 18–20*). Folding of the LDL-R to the native state involves the formation of 30 native disulfide bonds, each bridging stretches of up to 20 amino acids (*7, 10*). The large number of disulfide bonds and their domain-wise, local organization render the LDL-R a suitable model to determine whether such a large multidomain protein folds vectorially and/or cotranslationally and whether its domains fold independently in intact cells.

HeLa cells overexpressing human LDL-R were pulse-labeled for 5 min with ^{35}S-cysteine and ^{35}S-methionine and chased for 60 min in the absence of radioactivity. Detergent lysates of the cells were immunoprecipitated with a polyclonal antiserum recognizing virtually all conformations of the LDL-R, and analyzed by reducing SDS–polyacrylamide gel electrophoresis (SDS-PAGE) (*21*).

The LDL-R appeared as two bands (Fig. 1B), the lowest one at 120 kD (precursor form), which represents newly synthesized molecules in the ER. Correctly folded LDL-R passes ER quality control and is O-glycosylated in the Golgi complex to the 160-kD mature form (*22*). After 60 min of chase, a considerable fraction of LDL-R molecules had reached the Golgi form, but more than half still resided in the ER form.

When samples are denatured in the absence of reducing agent, a difference in SDS-PAGE mobility between nonreduced and the corresponding reduced samples indicates the presence of disulfide bonds. An alkylating agent is used to prevent postlysis formation and isomerization of disulfide bonds (*21*). Nonreduced and reduced immunoprecipitates were analyzed in adjacent lanes (Fig. 1C). The mature 160-kD form and the precursor 120-kD form of the denatured LDL-R both migrated at a higher mobility in the gel with intact disulfide bonds than in the corresponding reduced sample.

We exploited the differences in electrophoretic mobility between denatured oxidized and denatured reduced LDL-R to examine its folding process in the ER. To focus on the events in this compartment, we expressed the LDL-R by in vitro translation in the presence of semipermeabilized cells (*23*). Under these circumstances the LDL-R uses a relatively intact ER for folding but is not transported to the Golgi complex.

To prevent rapid oxidation of the LDL-R outside the ER and improve translocation efficiency, we translated the protein in the presence of 5 mM dithiothreitol (DTT) (Fig. 1D). After 30 min of translation, 15 mM oxidized glutathione was added, to allow oxidation of cysteines into disulfide bonds. The reduced full-length LDL-R band rapidly changed into a smear of folding intermediates with increasing gel mobility (Fig. 1D), suggesting immediate disulfide bond formation. After 30 min of glutathione incubation, the LDL-R started to accumulate in a single band with higher mobility than the reduced form (Fig. 1D), representing the native endpoint of folding. As expected, the 160-kD Golgi form did not appear, and all reduced samples had identical mobilities (Fig. 1E), confirming that all changes observed in the nonreducing gel were caused by changes in disulfide bonds. The mobility of all detectable folding intermediates after 5 min of chase was higher than that of the native endpoint; after an initial increase, their mobilities decreased again until the native state was reached (Fig. 1D).

The surprisingly small hydrodynamic volume of the first oxidative folding intermediates suggests the presence of large loops formed by disulfide bonding between distant cysteines. In the native protein, these long-range loops would be substituted for smaller intradomain loops of fewer than 20 amino acids, yielding a more extended molecule after denaturation (*21*). Thus, during productive LDL-R folding, long-range, presumably interdomain, non-native disulfide bonds isomerized into local intradomain native disulfides (fig. S2). This did not result in misfolding, because only a few aggregates were formed; folding to the native LDL-R was very efficient.

To confirm our findings in intact cells, we pulse-labeled HeLa cells overexpressing the LDL-R for 5 min in the presence of DTT to prevent oxidation during synthesis (*24*). The pulse was followed by a chase in the absence of DTT to restore the oxidative environment of the ER and allow the LDL-R to form disulfide bonds. The folding pattern in intact cells (Fig. 2A) was very similar to the pattern obtained in semipermeabilized cells (Fig. 1D); there was a fairly synchronized increase in mobility followed by a gradual decrease. Few aggregates appeared, which signified productive folding, and the folded forms passed ER quality control to become O-glycosylated in the Golgi complex, as indicated by the presence of the 160-kD form from 30 min on.

Compared to in vitro translation (Fig. 1, D and E), the intact cell showed one important difference: A discrete native 120-kD band was not present, most likely because properly folded native LDL-R was rapidly transported to the Golgi complex and O-glycosylated into the 160-kD form. The absence of O-glycosylation intermediates indicated that O-glycosylation occurred rapidly and efficiently. Folding, clearance by ER quality control, and transport of LDL-R molecules to the Golgi complex appeared highly asynchronous; the first, fastest maturing, molecules reached the Golgi complex after 30 min, the slowest more than an hour later (Fig. 2).

The folding processes studied here started with an artificially reduced LDL-R. Although folding could start during synthesis, disulfide bond formation was postponed until after synthesis, which synchronized the oxidative folding process. To determine whether disulfide bonds form during synthesis and whether this leads to the same abundance of non-

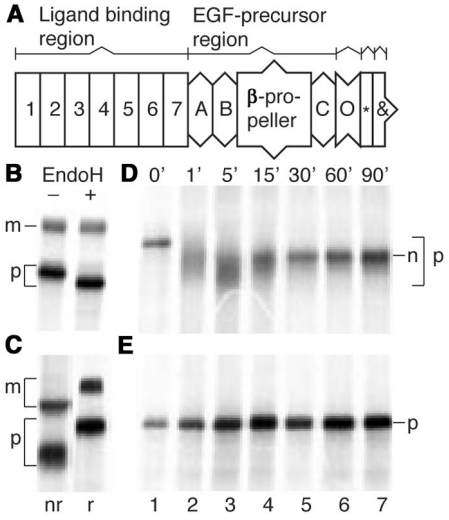

Fig. 1. (**A**) Domain organization of the LDL-R, which consists of five regions. The ligand-binding region contains seven ligand-binding domains, each stabilized by three disulfide bonds and a calcium ion. In the EGF precursor region, two EGF domains (A and B) are followed by a six-bladed β-propeller, flanked by a third EGF domain (C). Each EGF domain is stabilized by three disulfide bonds. In the native LDL-R, all disulfide-bonded loops present in the ligand-binding and EGF domains span a maximum of 20 amino acids. The other regions of the LDL-R—the O-glycosylation region (O), the transmembrane region (*), and the cytosolic tail (&)—do not contain any disulfide bonds. (**B** and **C**) Cells were pulse-labeled for 5 min, chased for 1 hour, and lysed in detergent (*21*). Cell lysates were immunoprecipitated with polyclonal antiserum. One-hour chase samples were treated with endoglycosidase H (Endo H) (+) or not (–), and subjected to reducing SDS-PAGE (B). The mobility of the 160-kD mature form did not change after Endo H treatment, confirming that it represented Endo H–resistant LDL-R that had left the ER and reached the medial Golgi complex. The 120-kD precursor was Endo H sensitive and localized to a pre-Golgi compartment. (C) Nonreduced (nr) and reduced (r) 1-hour chase immunoprecipitation samples were loaded in adjacent lanes. (**D** and **E**) Folding of the LDL-R after 30-min in vitro translation in the presence of DTT and semipermeabilized HT1080 cells; samples were taken at various time points after the addition of oxidized glutathione. Detergent lysates were immunoprecipitated with polyclonal antiserum. Samples were subjected to nonreducing (D) and reducing (E) SDS-PAGE. Lanes 1 to 3 were exposed to film for 7 days, the other lanes for 3 days. p represents the 120-kD precursor form, m represents the 160-kD mature form, and n represents the native 120-kD form.

native large-loop–forming disulfide bonds during folding, we studied LDL-R folding in the absence of DTT.

HeLa cells overexpressing the LDL-R were pulse-labeled for 5 min and chased for up to 2 hours. The folding pattern of the 120-kD form (Fig. 3A) was essentially the same as that of the later folding stages in Fig. 2A, with again a gradually decreasing mobility of the 120-kD form. However, the initial rapid mobility increase was absent. Instead, the first full-length folding intermediates had already acquired disulfide bonds during synthesis, implying substantial cotranslational oxidative folding in the protein (Fig. 3A). Because the completely reduced LDL-R precursor again did not change mobility with time (Fig. 3B), posttranslational modifications other than disulfide formation did not contribute to the decrease in mobility of nonreduced protein (Fig. 3A) (*21*). Results were the same for endogenously expressed LDL-R (fig. S1).

Although disulfide bond formation in the LDL-R does start during translation, proper folding of the protein does not begin with the formation of small loops within ligand-binding domains, but instead with large loops between distant cysteines (Fig. 3A and fig. S2). If the LDL-R were to fold from NH_2- to COOH-terminus, the first ligand-binding domain could already form cotranslationally. To examine this possibility, we immunoprecipitated the same lysates shown in Fig. 3, A and B, with monoclonal antibody (mAb) C7 (Fig. 3, C and D). This mAb recognizes a conformational epitope in the first NH_2-terminally located ligand-binding domain of 42 amino acids, provided the native disulfide bonds are present (*25–27*), irrespective of denaturation by SDS.

When compared to the polyclonal antiserum, mAb C7 reacted weakly with the newly synthesized LDL-R. It precipitated only a small fraction of the early folding intermediates, namely, those with lowest electrophoretic mobility (Fig. 3C and fig. S3) (*21*). The reduced samples (Fig. 3D) revealed the increased recognition by C7 with time (fig. S4). To exclude the possibility that the epitope was present in early folding intermediates but not accessible to the antibody, we treated lysates with 1% SDS at 95°C for 5 min before immunoprecipitation. C7 recognition did not change as a result of this treatment. Thus, the C7 epitope was formed late in the productive folding process of the LDL-R, although its NH_2-terminal location, in principle, would allow otherwise.

The ligand-binding domains in the LDL-R have been thought to fold independently of each other (*1–3, 12*); some isolated domains have been shown to fold properly in vitro (*7, 28*). Nevertheless, our results indicate that the first ligand-binding domain does not fold independently in intact cells, but instead first interacts with downstream residues during proper folding. Our most noteworthy observation was the abundance of LDL-R molecules that passed through high-mobility intermediates. The formation of non-native intrachain disulfide bonds during folding to the native state therefore is an intrinsic part of the folding pathway of this protein. This positions non-native disulfide bonds in the natural part of the folding pathway of a protein, in contrast to the usual negative associations with misfolding and aggregation. We have shown here that non-native intrachain disulfides are prominent in folding intermediates of an efficiently and correctly folding protein in intact cells.

Thus, the LDL-R does not fold vectorially, even though its domains are organized from NH_2- to COOH-terminus and it starts to fold during synthesis. Instead, non-native disulfide bonds form during productive folding of the LDL-R, most likely between cysteines of different domains (fig. S2). Aggregation is rare, and unscrambling of the intermediates into native protein occurs with high yield. Considering the similarity in domain structure between the members of the LDL-R family, we anticipate that our findings are relevant to a large set of biologically important proteins.

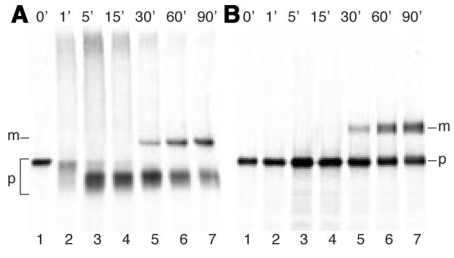

Fig. 2. Cells were pulse labeled in the presence of 10 mM DTT, and chased in the absence of DTT for up to 90 min. Samples, prepared as in Fig. 1, D and E, were subjected to nonreducing (**A**) and reducing (**B**) SDS-PAGE.

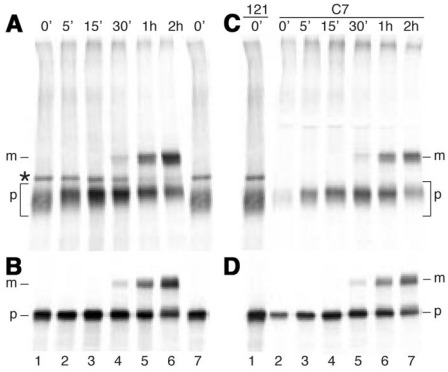

Fig. 3. Cells were pulse-labeled for 5 min, chased for up to 2 hours, and lysed in detergent. Cell lysates were immunoprecipitated with polyclonal antiserum (**A** and **B**) and in parallel with mAb C7 (**C** and **D**) (*21*). Samples were subjected to nonreducing [(A) and (C)] and reducing [(B) and (D)] SDS-PAGE. To emphasize the difference in mobility between early and late folding intermediates, the 0- and 2-hour chase samples are shown in adjacent lanes (A, lanes 7 and 6, respectively). Zero-min chase samples precipitated with polyclonal antiserum (C) (lane 1) are shown next to 0-min chase samples precipitated with mAb C7 (C) (lane 2). Exposure to x-ray film for almost 4 months did not reveal additional intermediates in lane 2. The asterisk (*) indicates an unidentified protein, not LDL-R, that was immunoprecipitated by the antiserum.

References and Notes

1. R. F. Doolittle, *Annu. Rev. Biochem.* **64**, 287 (1995).
2. R. Jaenicke, *Prog. Biophys. Mol. Biol.* **71**, 155 (1999).
3. W. J. Netzer, F. U. Hartl, *Nature* **388**, 343 (1997).
4. D. K. Strickland, S. L. Gonias, W. S. Argraves, *Trends Endocrinol. Metab.* **13**, 66 (2002).
5. M. M. Hussain, D. K. Strickland, A. Bakillah, *Annu. Rev. Nutr.* **19**, 141 (1999).
6. M. S. Brown, J. L. Goldstein, *Science* **232**, 34 (1986).
7. S. Bieri, J. T. Djordjevic, N. Jamshidi, R. Smith, P. A. Kroon, *FEBS Lett.* **371**, 341 (1995).
8. D. Fass, S. Blacklow, P. S. Kim, J. M. Berger, *Nature* **388**, 691 (1997).
9. H. Jeon *et al.*, *Nature Struct. Biol.* **8**, 499 (2001).
10. N. D. Kurniawan, K. Aliabadizadeh, I. M. Brereton, P. A. Kroon, R. Smith, *J. Mol. Biol.* **311**, 341 (2001).
11. N. D. Kurniawan *et al.*, *Protein Sci.* **9**, 1282 (2000).
12. C. L. North, S. C. Blacklow, *Biochemistry* **39**, 13127 (2000).
13. M. J. Gething, J. Sambrook, *Nature* **355**, 33 (1992).
14. L. Ellgaard, A. Helenius, *Curr. Opin. Cell Biol.* **13**, 431 (2001).
15. J. J. Ewbank, T. E. Creighton, *Biochemistry* **32**, 3677 (1993).
16. T. E. Creighton *et al.*, *J. Mol. Biol.* **232**, 1176 (1993).
17. B. van den Berg, E. W. Chung, C. V. Robinson, P. L. Mateo, C. M. Dobson, *EMBO J.* **18**, 4794 (1999).
18. D. M. Ferrari, H. D. Söling, *Biochem. J.* **339**, 1 (1999).
19. R. B. Freedman, P. Klappa, L. W. Ruddock, *EMBO Rep.* **3**, 136 (2002).
20. J. S. Weissman, P. S. Kim, *Nature* **365**, 185 (1993).
21. Materials and methods are available as supporting online material on *Science* Online.
22. R. D. Cummings *et al.*, *J. Biol. Chem.* **258**, 15261 (1983).
23. R. Wilson *et al.*, *Biochem. J.* **307**, 679 (1995).
24. I. Braakman, J. Helenius, A. Helenius, *EMBO J.* **11**, 1717 (1992).
25. A. Jansens, E. van Duijn, I. Braakman, data not shown.
26. U. Beisiegel, W. J. Schneider, J. L. Goldstein, R. G. Anderson, M. S. Brown, *J. Biol. Chem.* **256**, 11923 (1981).
27. T. O. Daniel, W. J. Schneider, J. L. Goldstein, M. S. Brown, *J. Biol. Chem.* **258**, 4606 (1983).
28. C. L. North, S. C. Blacklow, *Biochemistry* **38**, 3926 (1999).
29. We thank M. Jorgensen for the pGEM-LDLR construct; J. Defesche and S. Fouchier for discussions and reagents; R. Sitia, A. Benham, F. Pena, and members of the Braakman group for useful discussions and critical comments on the manuscript; and H. Tabak for support. Supported by The Netherlands Heart Foundation (grant 1997B205).

Supporting Online Material

www.sciencemag.org/cgi/content/full/298/5602/2401/DC1
Materials and Methods
SOM Text
Figs. S1 to S4
References and Notes

10 September 2002; accepted 7 November 2002